

An Improved Model for Water Wetting Prediction in Oil-Water Two-Phase Flow

Xuanping Tang^(*), Sonja Richter, and Srdjan Nesic
Institute for Corrosion and Multiphase Technology
Ohio University
342 West State Street
Athens, OH 45701

ABSTRACT

Internal pipeline corrosion is a serious concern for transportation pipelines in the oil and gas industry. Water wetting is an important aspect of internal corrosion of mild steel pipelines, since the steel will not corrode unless the water is in direct contact with it. A water wetting model considering oil and water properties, flow rates, water cut, etc., has been proposed previously. This model showed good agreement between experimental results and the water wetting predictions for a water-paraffinic model oil system. However, for crude oil systems, this model over-predicted water wetting leading to overestimation of corrosion in realistic flow system. Here, a new, improved water wetting prediction model is proposed. The new model includes the effect of the steel surface-fluid interactions in order to calculate the transition between oil and water wetting in oil-water two-phase flow, in addition to considering the interaction between the bulk turbulence and the surface tension, as was done in the original model. The new model significantly improves the prediction of the critical oil phase velocity required for full water entrainment of water, when compared to the original model. The new model has been verified with results from large scale (0.1 m ID) multiphase flow loop experiments as well as with results obtained using a doughnut cell – which is a benchtop multiphase flow apparatus. The verification included data obtained with different crude oils as well as with a model oil containing different surface active chemical.

Key words: Water wetting, corrosion, wettability, oil-water flow, mechanistic model

INTRODUCTION

Corrosion problems occur in every aspect of the oil and gas industry, from production and transportation to storage and refinery operations. One of the most common occurrences of corrosion is internal corrosion within transportation pipelines. In multiphase well streams, there is often water as well as

^(*) Currently at Westport Technology Center – Intertek, 6700 Portwest Dr., Houston, TX 77024, USA

©2013 by NACE International.

Requests for permission to publish this manuscript in any form, in part or in whole, must be in writing to NACE International, Publications Division, 1440 South Creek Drive, Houston, Texas 77084.

The material presented and the views expressed in this paper are solely those of the author(s) and are not necessarily endorsed by the Association.

many different corrosive species, such as hydrogen sulfide (H₂S), carbon dioxide (CO₂) produced or injected for secondary recovery, produced organic acids, as well as strong acids injected to reduce formation damage around the well or to remove scale.¹ Water plays a key role in the internal corrosion associated with wells and pipelines. Roughly, the likelihood of corrosion increases with increased fraction of the water phase in the produced fluids. Whenever water comes into contact with the internal wall of a pipeline, which is known as “water wetting”, there is a potential for internal corrosion of the mild steel wall. On the other hand, if the oil phase flows intensely enough to entrain the water phase, the internal wall of the pipeline can be continuously wetted by the oil phase, known as “oil wetting”, and the probability of corrosion is very small.

In order to properly predict the corrosion rate in pipelines, it is very important to know which liquid (water or oil) is in contact with the pipe wall and at what point all the water will be entrained by the oil, thereby eliminating corrosion within the pipeline. Cai et al.^{2,3} and Nesic et al.⁴ proposed an approach for predicting water-in-oil fully dispersed flow by extending and modifying the original work of Brauner⁵ and Barnea.⁶ The effects of flow velocity, oil and water properties (density, viscosity and interfacial tension), pipe diameter, pipe inclination, and water cut, on the critical oil velocity required for full water entrainment were considered in the model. This model was incorporated as a generic water wetting module in the mechanistic CO₂ corrosion prediction software package MULTICORP[†] produced by the Institute for Corrosion and Multiphase Technology (ICMT) at Ohio University.

THE PREVIOUS WATER-WETTING MODEL

In the original Brauner⁵ model, a unified approach was proposed for the prediction of dispersed flow pattern in gas-liquid and liquid-liquid systems. A criterion for transition from stratified to dispersed-flow based on a revised and extended Hinze's⁷ model was developed. Two physical properties are calculated and compared in order to determine whether the transition to dispersed flow pattern takes place: the maximum droplet diameter (d_{max}) calculated by Equation (1) and related to droplet breakup and coalescence, versus the critical droplet diameter (d_{crit}) as calculated by Equation (2) and related to droplet migration due to gravity ($d_{crit}^{gravity}$, Equation (3)), or deformation and swerving ($d_{crit}^{deformation}$, Equation (4)). When the maximum diameter is larger than the critical diameter, then the water would wet the pipe wall, and when the maximum diameter is smaller than the critical diameter, the water would be entrained and oil wetting is predicted. More detailed description of this model can be found in a prior publication.²

$$d_{max} = 2.22D \left(\frac{\rho_o D U_{so}^2}{\sigma} \right)^{-0.6} \left(\frac{\varepsilon_w}{1 - \varepsilon_w} \right)^{0.6} \left(\frac{\rho_m}{\rho_o (1 - \varepsilon_w)} f \right)^{-0.4} \quad (1)$$

$$d_{crit} = \min \left(d_{crit}^{gravity}, d_{crit}^{deformation} \right) \quad (2)$$

$$d_{crit}^{gravity} = \frac{3}{8} \frac{\rho_o f U_o^2}{|\Delta\rho| D g \cos \beta} \quad (3)$$

[†] Trade name

©2013 by NACE International.

Requests for permission to publish this manuscript in any form, in part or in whole, must be in writing to NACE International, Publications Division, 1440 South Creek Drive, Houston, Texas 77084.

The material presented and the views expressed in this paper are solely those of the author(s) and are not necessarily endorsed by the Association.

$$d_{crit}^{deformation} = \sqrt{\frac{0.4\sigma}{|\Delta\rho|g \cos \beta'}} \quad (4)$$

$$\beta' = \begin{cases} |\beta|, & |\beta| \leq 45^\circ \\ 90^\circ - |\beta|, & |\beta| > 45^\circ \end{cases} \quad (5)$$

The input parameters required for the model are the superficial oil velocity U_{so} (m/s), water cut ε_w (the volumetric ratio of water to the total liquid flow), the pipe diameter D (m), the inclination β ($^\circ$), the mixture density ρ_m (kg/m^3), which is a weighted average of the oil and water densities, the oil density ρ_o (kg/m^3), and the oil-water interfacial tension σ (N/m).

This water wetting model assumes that when the flow is intense enough to break up the water into small enough droplets so that they can be entrained by turbulence, oil wetting of the steel surface is always the correct outcome. Based on experimentation, this appeared to be true for “clean” systems which only involved pure water and a paraffinic model oil. However, when surface-active substances such as corrosion inhibitors or other chemicals were added into the oil-water system, the model consistently overestimated the flow velocity required for water entrainment and onset of oil wetting.⁸ The same was true for cases involving crude oils. After thorough analysis, it was concluded that the deviation of the model prediction from the experimental transition line was caused by the effect of steel surface wettability changes, which occurred due to adsorption of surface active compounds. The effect of steel surface wettability was not considered in this water wetting model, which focused exclusively on the bulk hydrodynamics. The newly developed model described below, sought to address this problem.

THE NEW IMPROVED WATER WETTING MODEL

In order to improve the prediction of the transition from water to oil wetting, particularly for cases when surface active substances such as corrosion inhibitors or other naturally occurring compounds are present in the oil-water flow, a new water wetting model that considers the effect of surface wettability is developed and proposed below.

Water Wetting Model Including Surface Wetting

Maximum droplet diameter.

In the previous water wetting model, the assumption is made that the turbulent kinetic energy of the oil phase is all used to disrupt the droplet coalescence of the dispersed water phase and to form separate droplets, *i.e.*, the kinetic energy of the turbulent phase is converted into the surface energy of the newly formed droplets.² There is an inherent assumption here that the water phase has already been lifted from the pipe surface and has been dispersed. However, this assumption neglects the interaction between the water and the steel surface. In other words, the previous model considers the change in oil-water surface energy but overlooks the change in oil-steel and water-steel surface energy. Considering the oil-steel and water-steel surface energy changes, a new assumption can be made that the kinetic energy of the oil phase is used to create new interfaces of any kind (oil-water, steel-water, steel-oil).

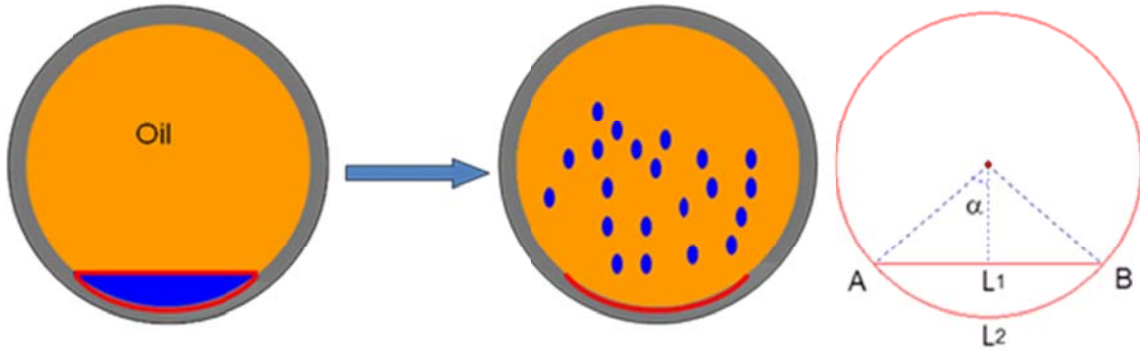


Figure 1: Schematic representation of transition from stratified flow to water-in-oil dispersion flow.

During the water to oil wetting transition, the surface energy changes can be separated into four parts, as described below. The first part (Equation (6)) represents the oil-water interfacial energy (considered in the previous model), while Equations (7-9) are new additions to the model. The parameters L_1 and L_2 are the length (m) of chord AB and arc AB in Figure 1, Q_w is the water flow rate (m^3/s), and σ_{os} and σ_{ws} (mN/m) represent the oil-steel interfacial tension and water-steel interfacial tension, respectively.

1. Surface energy gained from the newly formed oil-water interface:

$$E_{S1} = \frac{Q_w}{\pi d_{\max}^3 / 6} \cdot \pi d_{\max}^2 \cdot \sigma = \frac{6\sigma}{d_{\max}} Q_w \quad (6)$$

2. Surface energy lost from the eliminated oil-water interface, L_1 :

$$E_{S2} = -\frac{Q_w}{\varepsilon_w (\pi D^2 / 4)} \cdot L_1 \cdot \sigma = -\frac{L_1 Q_w}{\varepsilon_w (\pi D^2 / 4)} \sigma \quad (7)$$

3. Surface energy gained from the newly formed oil-steel interface, L_2 :

$$E_{S3} = \frac{Q_w}{\varepsilon_w (\pi D^2 / 4)} \cdot L_2 \cdot \sigma_{os} = \frac{L_2 Q_w}{\varepsilon_w (\pi D^2 / 4)} \sigma_{os} \quad (8)$$

4. Surface energy lost from the eliminated water-steel interface, L_2 :

$$E_{S4} = -\frac{Q_w}{\varepsilon_w (\pi D^2 / 4)} \cdot L_2 \cdot \sigma_{ws} = -\frac{L_2 Q_w}{\varepsilon_w (\pi D^2 / 4)} \sigma_{ws} \quad (9)$$

The total surface energy change listed above is proportional to the kinetic energy ($1/2 \rho_o \bar{v}^2 Q_o$) supplied by the continuous oil phase (Equation (10)), where \bar{v} is the mean velocity fluctuation and Q_o is the oil flow rate (m^3/s).

$$\frac{1}{2} \rho_o \bar{v}^2 Q_o \propto E_{S1} + E_{S2} + E_{S3} + E_{S4} = \frac{6\sigma Q_w}{d_{\max}} - \frac{L_1 \sigma Q_w}{\varepsilon_w (\pi D^2 / 4)} + \frac{L_2 \sigma_{os} Q_w}{\varepsilon_w (\pi D^2 / 4)} - \frac{L_2 \sigma_{ws} Q_w}{\varepsilon_w (\pi D^2 / 4)} \quad (10)$$

or

$$\frac{1}{2} \rho_o \bar{v}^2 Q_o = C_H Q_w \sigma \left(\frac{6}{d_{\max}} - \frac{4L_1}{\varepsilon_w \pi D^2} \right) + C_W Q_w \frac{4L_2}{\varepsilon_w \pi D^2} (\sigma_{os} - \sigma_{ws}) \quad (11)$$

From Equation (11), it can be seen that in this energy budget, the turbulent kinetic energy of the flow is used to make new water droplets as well as remove the water layer from the steel surface, *i.e.*, to create

new oil-steel interfaces. The constant in the new model C_H is set to 1, which is the same as what was used in the original model of Brauner.⁵ The new constant C_W is related to the fraction of the kinetic energy of turbulence consumed for creating the new oil-steel interfaces. The value of C_W can be estimated using experimental data involving surface active compounds, and is set to 30.

The fraction of the turbulent eddies which are most effective in breaking up the water droplets are those which are of the same length scale as the droplets. This is expressed by calculating the squared mean velocity fluctuation (Equation (12)) in terms of the rate of turbulent energy dissipation (Equation (13)).²

$$\bar{v}^2 = 2(\bar{e}d_{max})^{2/3} \quad (12)$$

$$\bar{e} = 2\rho_m U_{so}^3 f / \rho_o (1 - \varepsilon_w) D \quad (13)$$

The lengths L_1 (Equation (14)) and L_2 (Equation (15)) can be expressed in terms of the pipe diameter (D) and the angle α shown in Figure 1, based on geometrical calculations. Furthermore, the area of the free water layer, i.e., the water cut in stratified oil-water flow, is expressed by Equation (16).

$$L_1 = D \sin \alpha \quad (14)$$

$$L_2 = D \alpha \quad (15)$$

$$\varepsilon_w = \frac{2\alpha - \sin 2\alpha}{2\pi} \quad (16)$$

By applying Young's equation⁹ (Equation (17)) to Equation (11) one can get the maximum droplet diameter d_{max} (Equation (18)). The contact angle, θ , is the oil-in-water contact angle obtained experimentally by a goniometer by placing a water droplet on a oil pre-wetted steel surface.⁸

$$\sigma_{os} - \sigma_{ws} = \sigma \cos \theta \quad (17)$$

$$\left(\frac{d_{max}}{D} 2U_{so}^3 f \frac{\rho_m}{\rho_o (1 - \varepsilon_w)} \right)^{2/3} = \frac{\varepsilon_w \sigma}{\rho_o (1 - \varepsilon_w)} \left(C_H \left(\frac{6}{d_{max}} - \frac{4 \sin \alpha}{\varepsilon_w \pi D} \right) + C_W \frac{4\alpha \cos \theta}{\varepsilon_w \pi D} \right) \quad (18)$$

Since Equation (18) can not be solved algebraically for d_{max} , it needs to be solved numerically. This is done by finding the d_{max} that equals the d_{crit} (Equation (2)) for a given mixture velocity, $U_m = U_{so} + U_{sw}$ by changing the angle α . The water cut, ε_w , is then calculated using Equation (16).

Critical droplet diameter.

The critical droplet diameter due to gravity, $d_{crit}^{gravity}$, remains unchanged in the new model (Equation (3)). Brauner⁵ extended Brodkey's¹⁰ work by adding the effect of the pipeline inclination to calculate the critical droplet diameter $d_{critical}^{deformation}$ for deformation (Equation (4)). The idea is that a deformed droplet

will be unstable in the flow and start to swerve toward the pipe wall even in vertical flow. Brodkey's work was originally based on work done by Bond and Newton¹¹, who proposed a criterion using dimensional analysis to determine the critical radius of a bubble or droplet for the deviation from spherical shape. Brodkey had used the constant 0.4 in Equation (4) while Bond and Newton used the 4 (see Equation (19)). Since there was good agreement with the water in oil data in the original paper, Equation (19) is used instead of Equation (4) for the deformation critical droplet diameter.

$$d_{crit}^{deformation} = \sqrt{\frac{4\sigma}{|\Delta\rho|g \cos \beta'}} \quad (19)$$

Model Verification

Fluids and chemicals

Data for testing the model came from wetting maps generated by experiments conducted in a 0.1 m ID inclinable multiphase flow loop¹ and a benchtop apparatus called a “doughnut cell”.¹² The properties of the model oil and five different crude oils used in this study are given in Table 1, where they are ordered by increasing density and viscosity. The interfacial tension of the different crude oils is similar and considerably lower than the interfacial tension of the model oil.

The model was also verified for flow including a generic corrosion inhibitor (quaternary ammonium chloride)¹³ and a another case involving a model compound, myristic acid, which is a C14 carboxylic acid and has previously been found to have excellent corrosion inhibitive and oil wetting properties.^{14,15}

Table 1.
Properties of the oils used for verifying the model

Oil phase	Density, ρ (kg/m ³)	Dynamic viscosity, μ (mPa.S)	Interfacial tension, σ (mN/m)
Model Oil ^(‡)	825	2.0	40.0
Crude 1	778	1.6	25.2
Crude 2	830	4.7	26.2
Crude 3	853	9.1	28.1
Crude 4	879	22	23.2
Crude 5	890	36	26.5

[‡] LVT200TM (trade name)

©2013 by NACE International.

Requests for permission to publish this manuscript in any form, in part or in whole, must be in writing to NACE International, Publications Division, 1440 South Creek Drive, Houston, Texas 77084.

The material presented and the views expressed in this paper are solely those of the author(s) and are not necessarily endorsed by the Association.

Baseline test results

For the baseline test, the model oil, without any corrosion inhibitors or chemicals, was used as the oil phase in 0.1m horizontal oil-water pipe flow. The oil-in-water contact angle in 1 wt% NaCl was 73° .⁸ The transition lines to oil wetting predicted by the new model and the previous (old) model are compared with the empirical data in Figure 2. It can be seen that both models perform similarly well for the baseline test results.

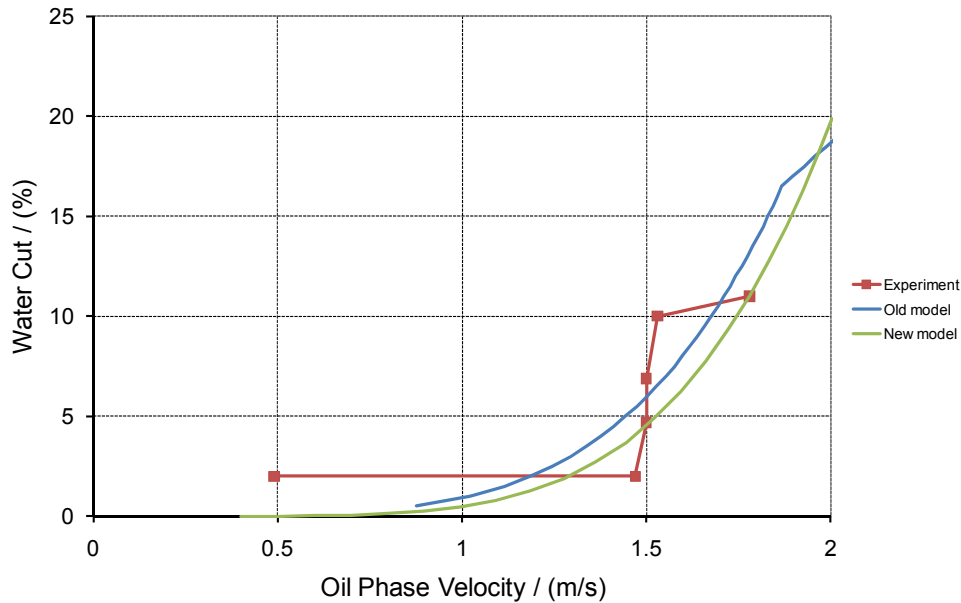


Figure 2: Comparison of model prediction results with experimental results from oil-water flow experiments conducted in a 0.1 m ID horizontal flow loop, (pure paraffinic model oil, contact angle: $\theta = 73^\circ$).

Results with crude oils

It was already reported that the previous (old) model over-predicted the critical oil phase velocity required for full water entrainment for different crude oils.⁸ By considering the effect of surface wettability, the new model significantly improves the accuracy of the prediction. This is demonstrated in Figure 3 to Figure 7, which show the comparison of model prediction results with experimental data obtained in a 0.1 m horizontal multiphase flow loop.

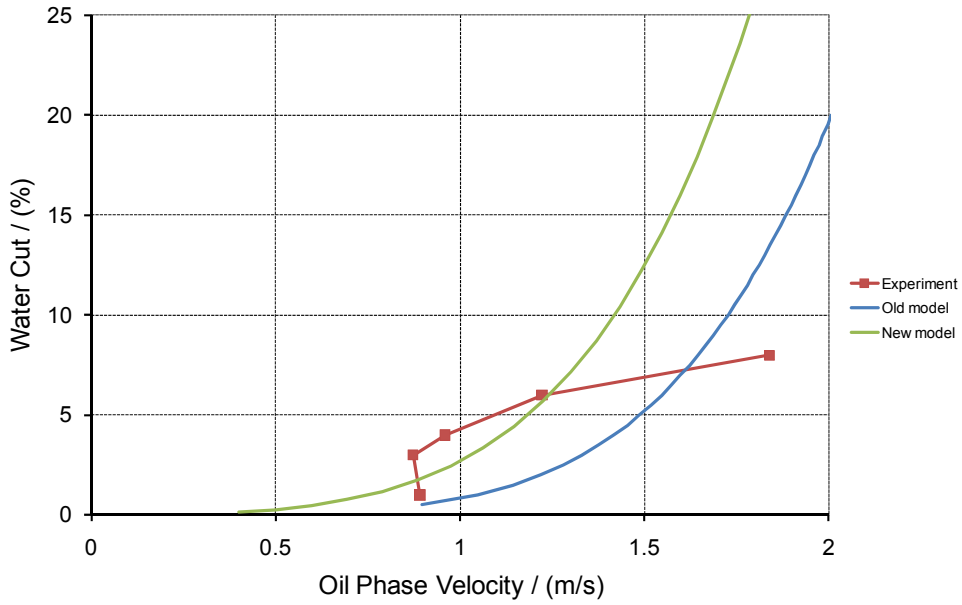


Figure 3: Comparison of model prediction results with experimental results from oil-water flow experiments conducted in a 0.1 m ID horizontal flow loop, (Crude oil 1, contact angle: $\theta=142^\circ$).

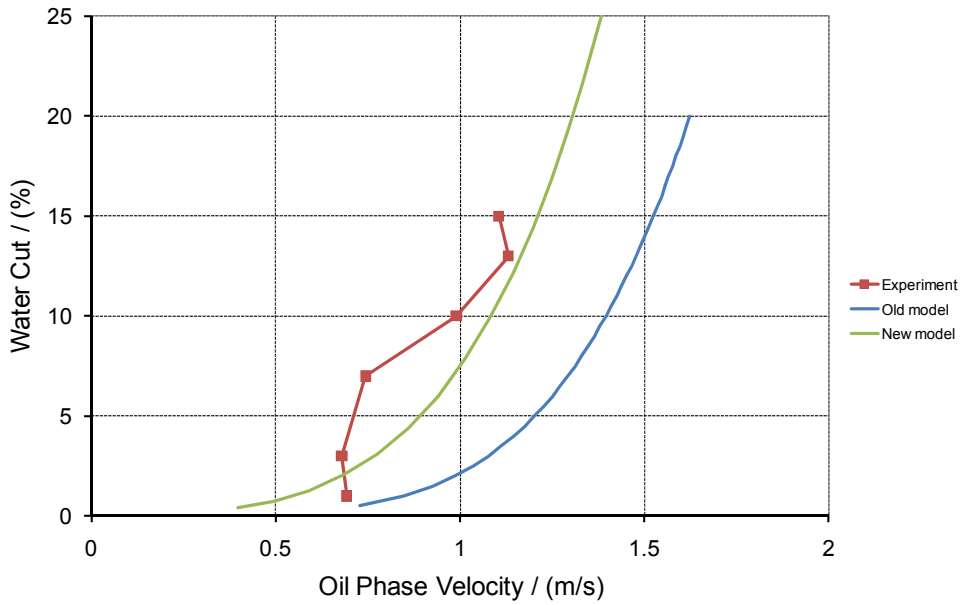


Figure 4: Comparison of model prediction results with experimental results from oil-water flow experiments conducted in a 0.1 m ID horizontal flow loop, (Crude oil 2, contact angle: $\theta=157^\circ$).

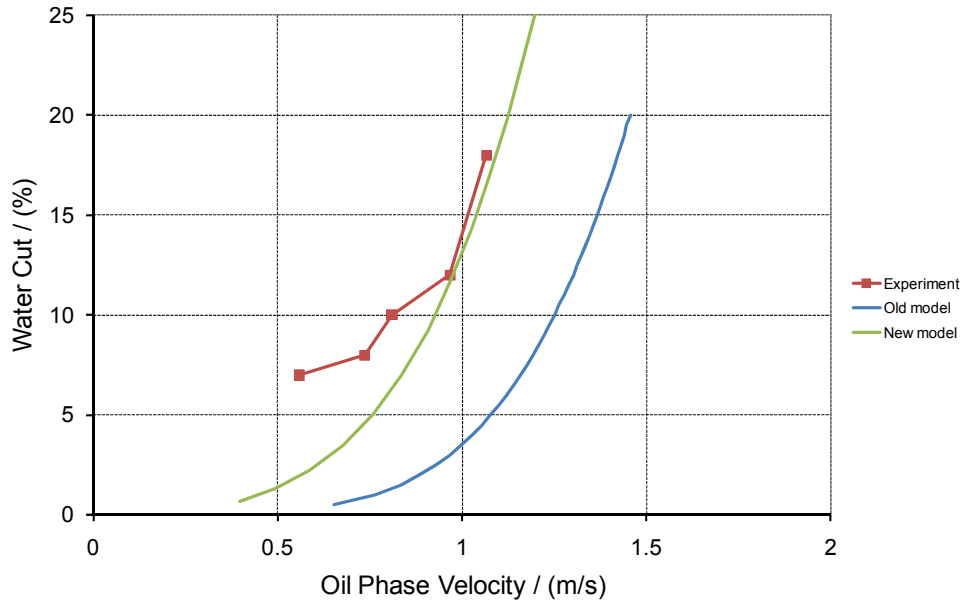


Figure 5: Comparison Comparison of model prediction results with experimental results from oil-water flow experiments conducted in a 0.1 m ID horizontal flow loop, (Crude oil 3, contact angle: $\theta=180^\circ$).

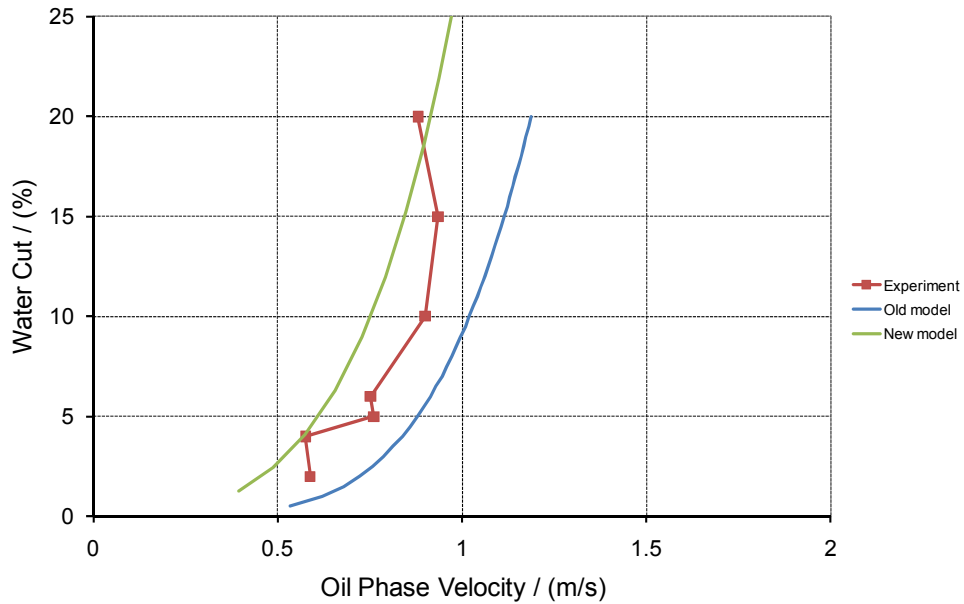


Figure 6: Comparison of model prediction results with experimental results from oil-water flow experiments conducted in a 0.1 m ID horizontal flow loop, (Crude oil 4, contact angle: $\theta=180^\circ$).

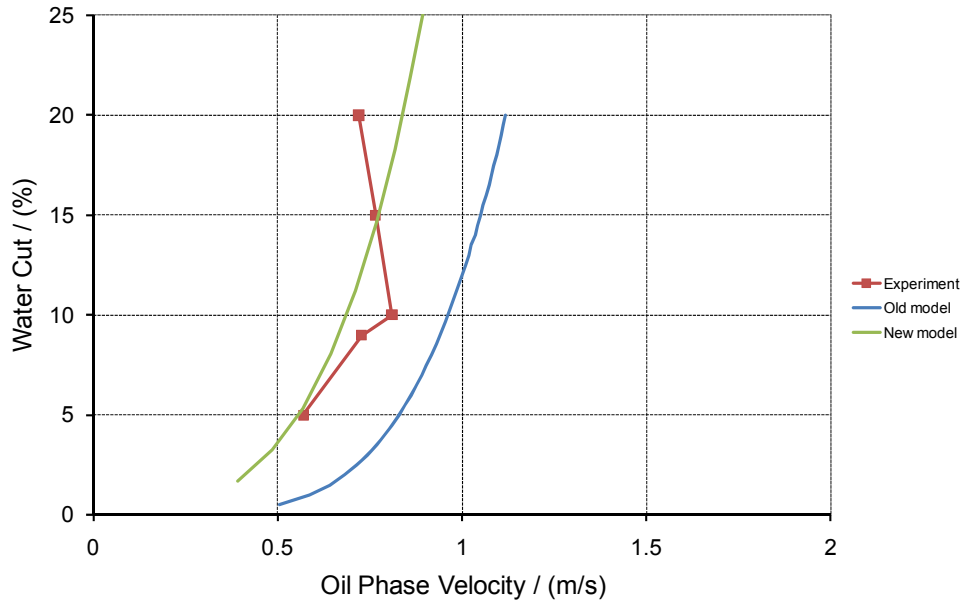


Figure 7: Comparison of model prediction results with experimental results from oil-water flow experiments conducted in a 0.1 m ID horizontal flow loop, (Crude oil 5, contact angle: $\theta=180^\circ$).

Results with corrosion inhibitor

The experimental data for a generic quaternary ammonium chloride inhibitor added to the water phase at different inhibitor concentrations (1 ppm, 5 ppm, 20 ppm) obtained by Li¹² in a doughnut cell were used to originally obtain C_w from Equation (18) based on the best fit. The experimental data obtained by Li in the doughnut cell were scaled up to a 0.1 m horizontal flow loop using the model described by Li.^{12,13} The oil-in-water contact angles for model oil on the steel surface pre-wetted with model oil in 1 wt% NaCl with 1 ppm, 5 ppm and 20 ppm quaternary ammonium chloride inhibitor added are 74°, 103°, and 151°, respectively.

Figure 8 shows the comparison of model prediction results with experimental results, for 1 ppm quaternary ammonium chloride inhibitor, tested in a doughnut cell and scaled up to a 0.1 m horizontal flow loop. Not much improvement is seen. However, for experiments with 5 ppm and 20 ppm inhibitor concentration (Figure 9 and Figure 10), it was found that new model results fits the experimental results much better. It can be seen that the old model over-predicts the critical oil velocity required for full water entrainment. A similar comparison is also made for experimental results obtained in a large scale 0.1 m flow loop for oil-water flow containing 5ppm quaternary ammonium chloride, as shown in Figure 11.

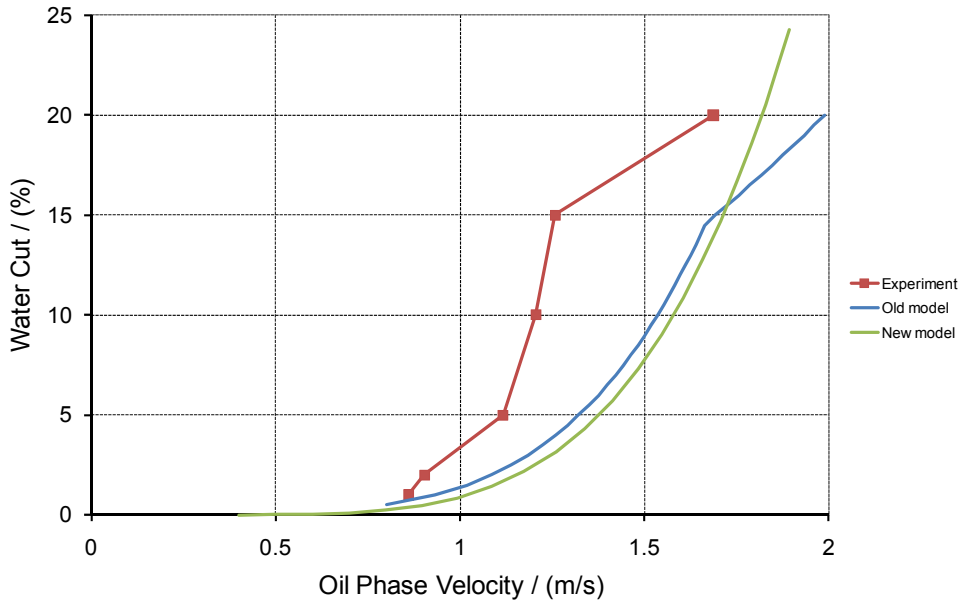


Figure 8: Comparison of model prediction results with experimental results obtained in oil-water flow in a doughnut cell scaled up to 0.1 m horizontal multiphase flow loop, (paraffinic model oil with 1 ppm quaternary ammonium chloride, contact angle: $\theta=74^\circ$).

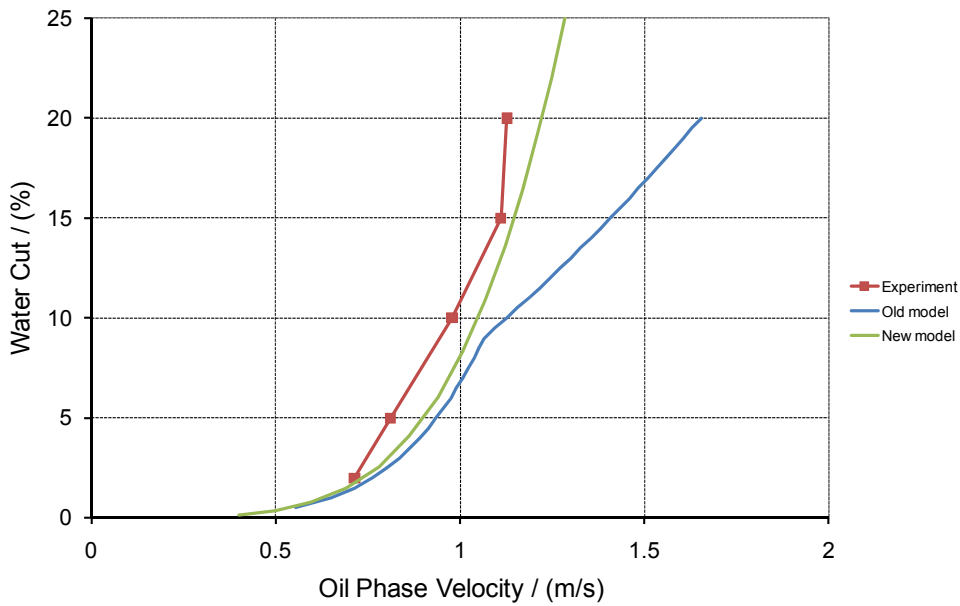


Figure 9: Comparison of model prediction results with experimental results obtained in oil-water flow in a doughnut cell scaled up to 0.1 m horizontal multiphase flow loop, (paraffinic model oil with 5 ppm quaternary ammonium chloride, contact angle: $\theta=103^\circ$).

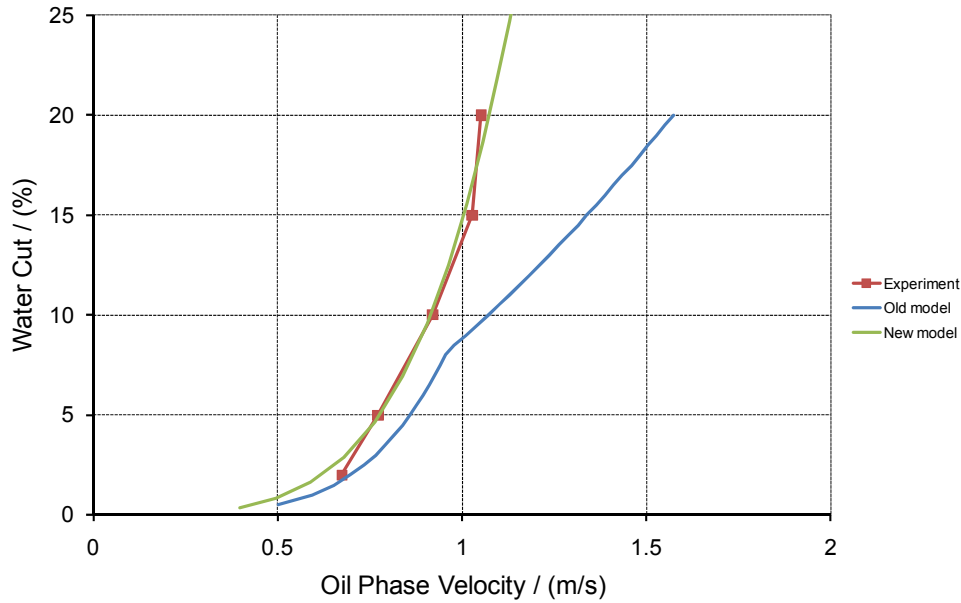


Figure 10: Comparison of model prediction results with experimental results obtained in oil-water flow in a doughnut cell scaled up to 0.1 m horizontal multiphase flow loop, (paraffinic model oil with 20 ppm quaternary ammonium chloride, contact angle: $\theta=151^\circ$).

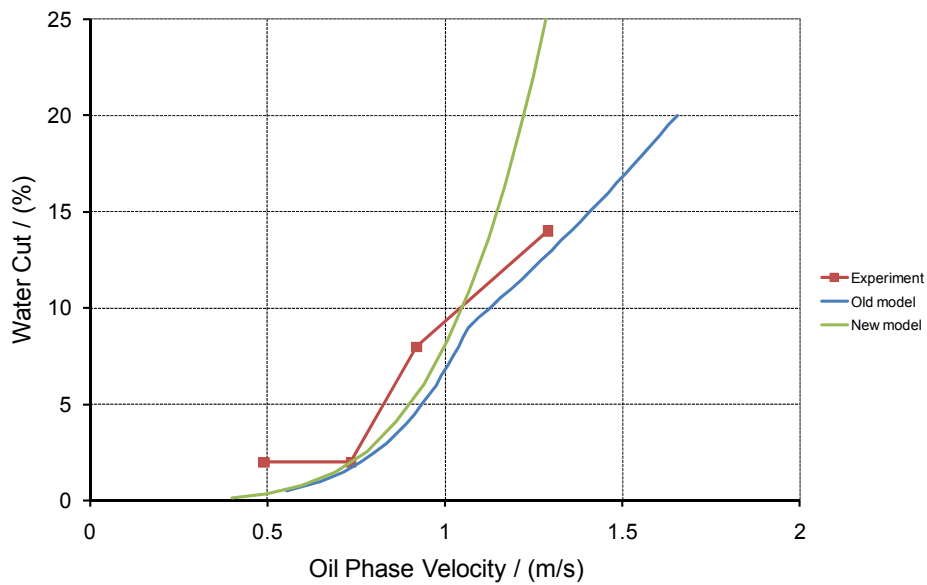


Figure 11: Comparison of model prediction results with experimental results from oil-water flow experiments conducted in a 0.1 m ID horizontal flow loop, (paraffinic model oil with 5ppm quaternary ammonium chloride, contact angle: $\theta=103^\circ$).

Results with surface active chemical additives

Figure 12 and Figure 13 show the comparison of model predictions with experimental results for model oil containing 0.01 wt% and 0.05 wt% myristic acid, respectively, obtained in oil-water flow in a 0.1 m horizontal multiphase flow loop.¹⁵ An improvement in prediction is obtained for both cases.

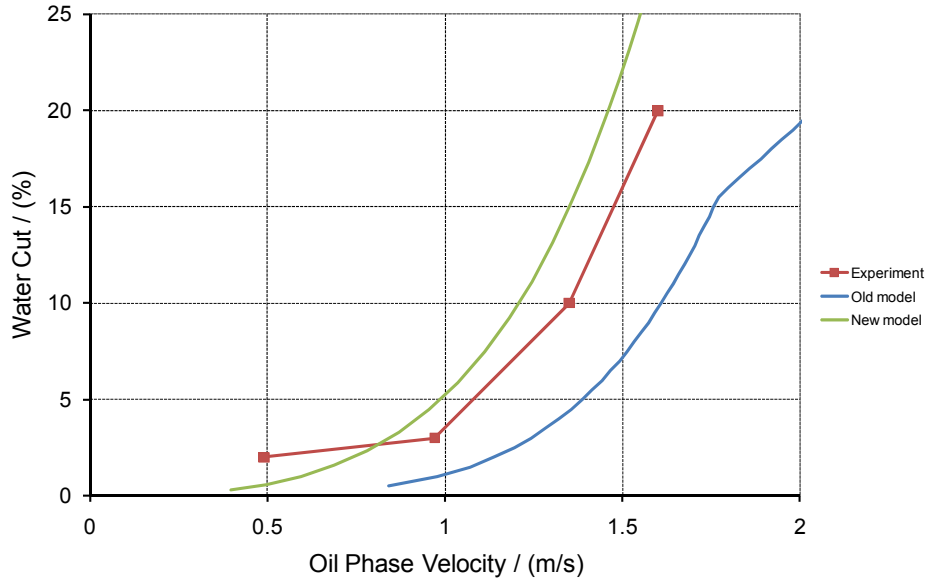


Figure 12: Comparison of model prediction results with experimental results from oil-water flow experiments conducted in a 0.1 m ID horizontal flow loop, (paraffinic model oil with 0.01 wt% myristic acid, contact angle: $\theta=180^\circ$).

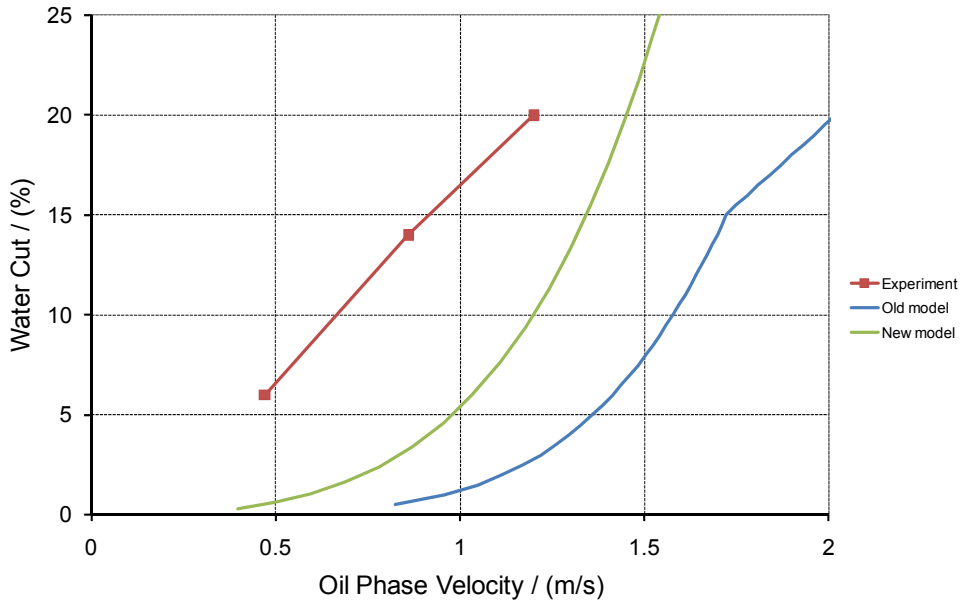


Figure 13: Comparison of model prediction results with experimental results from oil-water flow experiments conducted in a 0.1 m ID horizontal flow loop, (paraffinic model oil with 0.05 wt% myristic acid, contact angle: $\theta=180^\circ$).

CONCLUSIONS

A new water wetting prediction model that considers the effect of surface wettability has been proposed, based on the extension of a previous version of the model. The new model considers the effect of surface wettability in order to calculate the maximum water droplet size in oil-water flow. It is assumed that the turbulent kinetic energy of the oil phase is used to create new interfaces, which include oil-water interfaces and oil-steel interfaces. The new model can significantly improve the prediction of the critical oil phase velocity required for full water entrainment, which is verified by comparing with the experimental results using different crude oils and model oils containing surface active chemicals.

ACKNOWLEDGEMENTS

The financial support and technical directions from sponsoring companies: BP, ConocoPhillips, Eni, ExxonMobil, Petrobras, Saudi Aramco, Shell and Total are gratefully acknowledged.

REFERENCES

1. D. Brondel, R. Edwards, A. Hayman, D. Hill, S. Mehta, & T. Semerad, "Corrosion in the oil industry," *Oilfield Review*, 6(2) (1994): p. 4-18.
2. J. Cai, C. Li, X. Tang, F. Ayello, S. Richter, S. Nestic, "Experimental Study of Water Wetting in Oil-water Two Phase Flow-Horizontal Flow of Model Oil," *Chemical Engineering Science* 73, (2012): p.334-344.
3. J. Cai, S. Nestic, & C. de Waard, "Modeling of Water Wetting in Oil-water Pipe Flow," Corrosion/04, paper no. 04663, (Houston, TX, NACE, 2004).
4. S. Nestic, S. Wang, J. Cai, & Y. Xiao, "Integrated CO₂ Corrosion-multiphase Flow Model," Corrosion/04, Paper nr. 04626, (Houston, TX, NACE, 2004).
5. N. Brauner, "The Prediction of Dispersed Flows Boundaries in Liquid-liquid and Gas-liquid Systems," *International Journal of Multiphase Flow*, 27, (2001): p. 885-910.
6. D. Barnea, "A Unified Model for Predicting Flow-pattern Transitions for the Whole Range of Pipe Inclinations," *International Journal of Multiphase Flow*, 13, (1987): p. 1-12.
7. J. Hinze, "Fundamentals of the Hydrodynamic Mechanism of Splitting in Dispersion Processes," *AIChE Journal*, 1(3), (1955): p. 289-295.
8. X. Tang, "Effect of Surface State on Water Wetting and Carbon Dioxide Corrosion in Oil-water Two-phase Flow," Doctoral Dissertation, (2011), Ohio University.
9. T. Young, "An Essay on the Cohesion of Fluids," *Philosophical Transactions of the Royal Society of London*, 95, (1805): p.65-87.
10. R.S. Brodkey, *The phenomena of fluid motions*. (Reading, MA: Addison-Wesley, 1967).
11. W.N. Bond & D.A. Newton, "Bubbles, drops, and Stokes' law," *Philosophy Magazine*, 5, (1928): p. 794-800.
12. C. Li, S. Richter, S. Nestic, *How do Inhibitors Mitigate Corrosion in Oil-Water Two Phase Flow Beyond Lowering the Corrosion Rate?*, Corrosion/13, Paper nr. C2012-0002391, (Houston, TX, NACE, 2013).
13. C. Li, "Effect of Corrosion Inhibitor on Water Wetting and Carbon Dioxide Corrosion In Oil-Water Two-Phase Flow," Doctoral Dissertation, (2009), Ohio University.
14. F. Ayello, W. Robbins, S. Richter, S. Nestic, *Crude Oil Chemistry Effects on Inhibition of Corrosion and Phase Wetting*, Corrosion/11, Paper nr. 11060, (Houston, TX, NACE, 2011).
15. F. Ayello, "Crude Oil Chemistry Effects on Corrosion Inhibition and Phase Wetting in Oil-Water Two-Phase Flow," Doctoral Dissertation, (2010), Ohio University.